

IMOT: General-Purpose, Fast and Robust Estimation for Spatial Perception Problems with Outliers

Lei Sun¹

Abstract—Spatial perception problems are the fundamental building blocks of robotics and computer vision. However, in many real-world situations, they inevitably suffer from the issue of *outliers*, which hinders traditional solvers from making correct estimates. In this paper, we present a novel, general-purpose robust estimator IMOT (Iterative Multi-layered Otsu’s Thresholding) using standard *non-minimal* solvers to rapidly reject outliers for spatial perception problems. First, we propose a new outlier-robust iterative optimizing framework where in each iteration all the measurement data are separated into two groups according to the *residual errors* and only the group with lower residual errors can be preserved for estimation in the next iteration. Second, we introduce and employ the well-known Otsu’s method (from image processing) to conduct thresholding on the residual errors so as to obtain the best separation (grouping) statistically which maximizes the between-class variance. Third, to enhance robustness, we design a multi-layered Otsu’s thresholding approach in combination with our framework to sift out the true inliers from outliers that might even occupy the majority of measurements. We test our robust estimator IMOT on 5 different spatial perception problems including: rotation averaging, rotation search, point cloud registration, category-level registration, and SLAM. Experiments show that IMOT is robust against 70%–90% of outliers and can typically converge in only 3–10 iterations, being 3–125 times faster than existing robust estimators: GNC and ADAPT. Moreover, IMOT is able to return robust results even without noise bound information.

I. INTRODUCTION

Spatial perception problems, which seek to estimate the geometric models regarding the state of a robot and its relation to the surroundings [27], are the crucial tasks in robotics and computer vision, and have found broad applications in motion estimation [33], object or camera localization [28], [32], 3D scene reconstruction [3], [8], SLAM [6], etc.

Unfortunately, in many real-world applications, in addition to the noise of devices, spatial perception problems are often jeopardized (negatively influenced) by the *outliers*, which are the spurious measurements probably caused by repetitive patterns, extreme noise, wrong data association, apparatus malfunction, etc, making traditional estimation methods very brittle and prone to fail.

To deal with the outlier issue, RANSAC [12] is the most popular robust estimator extensively applied in many perception problems to perform outlier rejection by incorporating the *minimal* solvers into a hypothesize-and-check paradigm. Though some variants (e.g. [9], [10], [25]) are rendered to improve the performance, RANSAC-type estimators are usually confronted with exponentially increasing computational

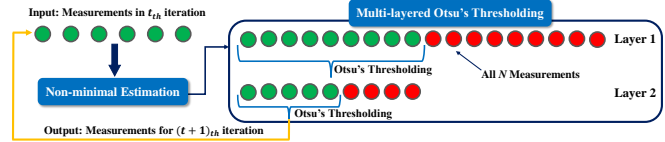


Fig. 1. An intuitive illustration of the proposed robust estimator IMOT. cost w.r.t. the outlier ratio and the problem dimension (size of the minimal subset), impractical for use in some realistic cases. Besides, minimal solvers are not always available or suitable in some problems (e.g. SLAM, category-level perception).

More currently, global general-purpose robust estimators: GNC [29] and ADAPT [27] are proposed to reject outliers directly in conjunction with standard *non-minimal* solvers, which have caught increasing attention for use these years (e.g. [22] for SLAM, [30] for 2D-3D shape reconstruction, and [24] for category-level perception).

Though GNC and ADAPT can reject 70%–80% outliers in multiple problems, they generally seem too slow to converge, mostly requiring dozens of, or even over a hundred, iterations to reach convergence. As many non-minimal solvers are not as fast as minimal ones, the gain of robustness using GNC and ADAPT may in turn result in much longer solution time.

Therefore, in order to address the slow-convergence problem in the non-minimal robust estimation, this paper provides a novel general-purpose robust estimator named IMOT (Iterative Multi-layered Otsu’s Thresholding) that is able to converge within only several (3–10) iterations while demonstrating robustness comparable to (sometimes even superior to) GNC and/or ADAPT. Moreover, the proposed estimator can also adapt to inlier-threshold-free conditions with similar robustness, showing high flexibility for use when the inlier-noise statistics are unknown. Finally, we showcase our robust estimator in 5 different spatial perception problems: single rotation averaging, rotation search, point cloud registration, category-level perception, and SLAM, and demonstrate that our estimator is robust against 70%–90% outliers, is 3–125 times faster than GNC and/or ADAPT, and can outperform RANSAC and other specialized solvers in a number of cases.

II. RELATED WORK

A. Non-robust Estimation Methods

Minimal solvers can make estimates with only a few measurements (usually fewest measurements possible), and typical instances include: 2-point method [18] for rotation search, Horn’s triad-based method [14] for point cloud registration, 5-point solver [19] for two-view geometry. However,

*This work was not supported by any organization

¹Lei Sun is with School of Mechanical and Power Engineering, East China University of Science and Technology, Shanghai 200237, China, leisun_james@126.com

due to the absence of redundant measurements to refine the solution, minimal solvers could be easily affected by noise. Besides, some problems are unsuitable to be solved by minimal solvers because they have too many variables to solve (e.g. SLAM, category-level perception), making the dimension (number of measurements required) of the minimal solvers too high and thus significantly slowing down the RANSAC [12] process during outlier rejection.

Non-minimal solvers can usually take an arbitrary number of measurements (as long as the problem is overdetermined) as the input to estimate the solution by using least-squares methods under the assumption of Gaussian noise. Some typical examples include: Arun’s SVD method [2] for point cloud registration, Semi-Definite relaxation methods for 3D registration [4], category-level perception [24] and pose graph optimization [22], and Sum-of-Squares relaxation methods for 2D-3D shape alignment [29] and shape reconstruction [30]. Though non-minimal solvers can minimize the influence of noise and yield optimal results, they may suffer from relatively long runtime since the relaxation techniques on high-degree polynomial optimization usually necessitate high computational cost. So, once combined with the outlier rejection frameworks (e.g. GNC [29], ADAPT [27]) where plenty of iterations are required, the runtime problem of non-minimal solvers would appear critical.

B. Outlier-robust Estimation Methods

Consensus maximization realizes robust estimation by seeking the solution model that enables the largest number of measurements to have residual errors below the preset noise bound of inliers. RANSAC [12] is the most common consensus maximizer which repetitively takes random small measurement subsets to make minimal estimates for the solution and finds the best estimate that corresponds to the largest consensus set of the measurements. Additional techniques like local optimization [10] or measurement ranking [9] are also applied to improve RANSAC. But RANSAC solvers’ exponential runtime with the growth of the outlier ratio and problem dimension makes them too time-consuming for use in some practical situations. Branch-and-Bound [16] is another consensus maximization paradigm that can return globally optimal results, but BnB is also plagued by the worst-case exponential time w.r.t. the problem size. In addition, ADAPT [27] can reject outliers by alternating between non-minimal estimation and measurement trimming with a gradually decreasing residual threshold. But its downside is: ADAPT often requires at least dozens of iterations for convergence, but given the slowness of some non-minimal solvers, time-efficiency could be tremendously compromised.

M-estimation leverages robust cost functions to diminish the weights of outliers. Earlier local M-estimation methods [17] typically require an initial guess and iteratively optimize until convergence, but they are liable to be trapped in local minimum if the initial guess is poor. More recently, Graduated Non-Convexity (GNC) is presented to avoid the demand for the initial guess. GNC is first used in FGR [34] for robust point cloud registration. Then, Yang et al. promote

GNC as a general-purpose estimator for various perception problems [29]. But GNC also needs 25–50 iterations to converge, hence facing the same runtime issue as ADAPT.

III. IMOT: ITERATIVE MULTI-LAYERED OTSU’S THRESHOLDING

A. Generalized Problem Formulation for Spatial Perception

To describe the spatial perception problems in a general way, we adopt the formulation in [29]. Assume we have an estimation problem where the variables to estimate can be written as $\mathbf{x} \in \mathcal{X}$ and \mathcal{X} is the feasible domain of \mathbf{x} (e.g. if \mathbf{x} denotes the rotation matrix, \mathcal{X} should denote $SO(3)$), the N measurements of the problem are represented by \mathbf{m}_i , $i = 1, 2, \dots, N$ (e.g. if the problem is point cloud registration, \mathbf{m}_i should denote the correspondences across point clouds), and $Re(\mathbf{m}_i, \mathbf{x})$ represents the function that measures the extent of difference between the measurement computed with \mathbf{x} and the actual measurement \mathbf{m}_i (in addition, for a certain \mathbf{x} , $Re(\mathbf{m}_i, \mathbf{x})$ can also represent the *residual error* w.r.t. measurement \mathbf{m}_i , written as Re_i in the rest of the paper). Thus, in the ideal case where no outlier exists, this problem can be formulated as the following minimization problem:

$$\min_{\mathbf{x} \in \mathcal{X}} \sum_{i=1}^N Re^2(\mathbf{m}_i, \mathbf{x}). \quad (1)$$

Nonetheless, when outliers corrupt the measurements \mathbf{m}_i , the robust estimation for this problem can be written into a consensus maximization formulation [26], [27] such that

$$\begin{aligned} & \max_{\mathcal{I} \subset \mathcal{N}} |\mathcal{I}|, \\ & s.t. |Re(\mathbf{m}_i, \mathbf{x}^*)| \leq \gamma, (\forall i \in \mathcal{I}) \end{aligned} \quad (2)$$

where we aim to find the optimal solution \mathbf{x}^* that enables as many measurements \mathbf{m}_i as possible to have residual errors lower than the preset threshold (called noise bound) γ which is used to differentiate inliers from outliers, and here set \mathcal{I} , a subset of the full measurement set $\mathcal{N} = \{1, 2, \dots, N\}$, is called the consensus set w.r.t. the solution \mathbf{x}^* .

B. Iterative Grouping and Estimation: A Framework for Outlier Rejection

We propose an iterative outlier-rejective framework whose ultimate goal is to find one subset of the full measurement set that only comprises true inliers (though not all). In each iteration, this framework is operated by: (i) using a portion of the measurements to make a non-minimal estimate, and (ii) computing the residual errors to select the measurements that can be used for non-minimal estimation in the next iteration. Now we provide the explicit elaboration on it as follows.

In the t_{th} iteration, assuming we have a subset of the full measurement set: $\mathcal{C}^{t-1} \subset \mathcal{N}$ (computed in the $(t-1)_{th}$ iteration) as the input, we can first make an estimate on \mathbf{x}^t with the measurements in \mathcal{C}^{t-1} using a standard non-minimal solver, and then compute the residual errors $Re_i = Re(\mathbf{m}_i, \mathbf{x}^t)$ with the corresponding \mathbf{m}_i and the current \mathbf{x}^t .

Subsequently, through multiple empirical experiments, we find that: if we only pick out the measurements whose

residual errors are small enough from the full measurement set, gather them into set \mathcal{C}^t as the input for the $(t + 1)_{th}$ iteration and continue the iterations, we will be able to obtain a certain subset \mathcal{C}^u (in the u_{th} iteration) that is made up of true inliers only. In other words, the true inliers can gradually move into the low-residual subset as this iterative framework goes on. However, the main challenge in this framework is that: *how many or which low-residual measurements should be chosen for the next iteration each time?*

In real scenes, the actual statistics of the residual errors could change with many factors, e.g. application condition, type of problem, noise level, etc, which makes it fairly difficult to appropriately select the low-residual measurements, hence leading to poor (non-robust) results. Consequently, the next step is to find a general-purpose way to realize proper selecting of the low-residual measurements in each iteration.

C. Applying Otsu's Method for Residual Thresholding

Otsu's method [20] is a widely-used approach for image thresholding by grouping all the image pixels into two classes in a way that maximizes the between-class variance. In this work, we transplant Otsu's method to the thresholding of the residual errors in our framework, in order to accomplish automatic thresholding regardless of the statistic distribution.

According to [20], the intensity values of image pixels are typically integers ranging from 0 to 255, which facilitates the establishment of the intensity histogram. Thus, in each iteration of our framework, we should: (i) create a limited number of consecutive *intervals* to contain all the residual errors, and (ii) assign the residual errors to respective intervals that they lie into so as to construct the histogram on residual errors.

Specifically, we set the maximum residual error as the upper-bound of intervals such that $H^{max} = \max(Re_i), i = 1, 2, \dots, N$, and then split H^{max} into L consecutive small intervals where each interval has the same length equal to $\Delta H = \frac{H^{max}}{L}$ (Usually, we set $L = 200$ in practice). Hence, there exist L intervals which can be represented as: $(0, \Delta H], (\Delta H, 2\Delta H], (\Delta H, 2\Delta H], \dots, (H^{max} - \Delta H, H^{max}]$.

Then, we let $n_l (l = 1, 2, \dots, L)$ denote the number of residual errors that fall into the l_{th} interval, so that obviously $\sum_{l=1}^L n_l = N$. Following the routine of Otsu's method [20], we normalize n_l as $p_l = \frac{n_l}{N}$, so the probability for a random residual error to be lower than $k \cdot \Delta H$ can be given by:

$$P_k = \sum_{l=1}^k p_l, \quad (3)$$

where k is an integer ranging from 1 to L . The cumulative mean of residual errors lower than $k \cdot \Delta H$ can be written as:

$$\mu_k = \sum_{l=1}^k l \cdot p_l, \quad (4)$$

By letting $k = L$, we have the mean of all residual errors:

$$\bar{\mu} = \mu_L = \sum_{l=1}^L l \cdot p_l. \quad (5)$$

Up to now, the between-class variance for a certain $k (k = 1, 2, \dots, L)$ can be computed as:

$$\eta_k = \frac{(\bar{\mu}P_k - \mu_k)^2}{P_k(1 - P_k)}. \quad (6)$$

As a result, the best threshold \hat{T} here can be solved by:

$$\hat{T} = \Delta H \cdot \hat{k} = \Delta H \cdot \arg \max_{k=1,2,\dots,L} (\eta_k). \quad (7)$$

With the best \hat{T} computed above, we are able to separate all the measurements into two groups based on their residual errors as: a lower-residual group \mathcal{G}_α with residual errors no larger than $\hat{T} (\forall i \in \mathcal{G}_\alpha, Re_i \leq \hat{T})$, and a higher-residual group \mathcal{G}_β with residual errors larger than $\hat{T} (\forall i \in \mathcal{G}_\beta, Re_i > \hat{T})$. In this case, we can let the lower-residual group \mathcal{G}_α be the input set (\mathcal{C}^{t+1}) for the next iteration.

However, when the outlier ratio becomes higher (e.g. $> 50\%$), grouping the residual errors merely using the method above may also include outliers into the lower-residual group \mathcal{G}_α , preventing us from correctly sifting out the true inliers. Therefore, we need to further render a multi-layered Otsu's method to enhance the robustness of our framework.

D. Multi-layered Otsu's Thresholding to Boost Robustness

To make our framework robust against more outliers, we design an effective approach to progressively refine the lower-residual group via multiple layers (times) of Otsu's thresholding, so as to increase the possibility that only true inliers are preserved at the end of our framework.

Following Section III-C, after we finish the thresholding of all the residual errors with threshold \hat{T}^1 to achieve the lower-residual group \mathcal{G}_α^1 (here, superscript j denotes that \mathcal{G}_α^j and \hat{T}^j are obtained in the j_{st} layer of thresholding), we can further conduct another time of thresholding on \mathcal{G}_α^1 , which means that we can treat all the measurements in the current lower-residual group \mathcal{G}_α^1 as the input, and apply Otsu's thresholding once again to further separate \mathcal{G}_α^1 into two groups: \mathcal{G}_α^2 and \mathcal{G}_β^2 by a new threshold \hat{T}^2 estimated from (7).

In this manner, if we conduct d layers of Otsu's two-group thresholding (where d is a parameter preset by user before the algorithm), the lower-residual group in the last layer, written as \mathcal{G}_α^d , can be then taken as the input subset for the non-minimal estimation in the next iteration, and the threshold in the last layer \hat{T}^d would serve as the ultimate threshold in this iteration of our framework, written as: $T^t \leftarrow \hat{T}^d$.

Subsequently, looking back to the main framework in Section III-B, this multi-layered residual error thresholding and measurement grouping procedure will be repeated continuously in more iterations until the ultimate thresholds in 2 consecutive iterations (say T^t and T^{t-1}) are sufficiently close, e.g. $|T^t - T^{t-1}| \leq \delta$ (δ is small enough, e.g. $5e - 3$), where can we consider this framework to be converged.

E. Main Algorithm

So far, our algorithm can be described as: (i) iteratively grouping the measurements and taking the low-residual ones for non-minimal estimate in the next iteration (Section III-B),

Algorithm 1: IMOT* (without noise bound)

Input: measurements $\{\mathbf{m}_i\}_{i=1}^N$, number of layers for Otsu's thresholding d , convergence criterion δ ;

- 1 Set $\mathcal{N} \leftarrow \{1, 2, \dots, N\}$, $\mathcal{C}^0 \leftarrow \mathcal{N}$, and $L \leftarrow 200$;
- 2 **for** $t = 1 : 50$ **do**
- 3 Solve \mathbf{x}^t using the non-minimal solver with the measurements in set \mathcal{C}^{t-1} ;
- 4 Compute the residual errors Re_i w.r.t. all the measurements \mathbf{m}_i ;
- 5 $H^{max} \leftarrow \max(Re_i), \forall i \in \mathcal{N}$, $\Delta H \leftarrow \frac{H^{max}}{L}$;
- 6 Create L intervals and count n_l for all intervals;
- 7 $\mathcal{G}_\alpha^0 \leftarrow \mathcal{N}$, $\hat{T}^0 \leftarrow L$;
- 8 **for** $j=l:d$ **do**
- 9 For all $l \in [1, \frac{\hat{T}^{j-1}}{\Delta H}]$, compute $p_l \leftarrow \frac{n_l}{|\mathcal{G}_\alpha^{j-1}|}$;
- 10 For all $k \in [1, \frac{\hat{T}^{j-1}}{\Delta H}]$, update $P_k, \mu_k, \bar{\mu}$ and η_k according to (3)–(6);
- 11 Estimate the threshold \hat{T}^j based on (7) to separate \mathcal{G}_α^{j-1} into 2 groups: \mathcal{G}_α^j and \mathcal{G}_β^j ;
- 12 **end**
- 13 $T^t \leftarrow \hat{T}^d$ and $\mathcal{C}^t \leftarrow \mathcal{G}_\alpha^d$;
- 14 **if** $|T^t - T^{t-1}| \leq \delta$ **then**
- 15 **break**
- 16 **end**
- 17 **end**
- 18 **return** optimal solution $\mathbf{x}^* \leftarrow \mathbf{x}^t$ and inlier set \mathcal{C}^t ;

which continues until convergence, (ii) using multi-layered Otsu's method for thresholding and grouping in each iteration of step (i) (Section III-C to III-D), as illustrated in Fig. 1.

The proposed algorithm have 2 versions. The first version, named IMOT* (Algorithm 1), is the flexible version, in which we do not require any preset noise bound (inlier threshold) and the solution \mathbf{x}^t in the last iteration is directly returned as the optimal result when IMOT* converges, designed for situations where the noise data are unavailable. The second version IMOT (Algorithm 2) has the noise bound γ as input and can further refine the inlier set with γ after Algorithm 1. If the solved threshold T^t is much larger than γ , say $T^t \geq 5\gamma$, we use an iterative optimization technique (inspired by [10]) where the inlier set \mathcal{E} and solution \mathbf{x} are alternately solved with the inlier threshold decreasing from T^t to γ gradually; if not, we refine the inlier set directly using γ as the threshold.

In terms of the recommended choice of the layer number of thresholding d , we suggest: $d = 2$ if $N < 200$, $d = 3$ if $N \geq 200$, and $d = 4$ for SLAM (regardless of N). And the convergence criterion can be set as: $\delta = 5e - 3$ in practice.

IV. EXPERIMENTS AND APPLICATIONS

We demonstrate our robust estimator IMOT (and IMOT*) in 5 spatial perception problems: single rotation averaging, rotation search, point cloud registration, category-level perception, and SLAM. We benchmark our estimator with the state-of-the-art general-purpose robust estimators: (i) GNC-TLS and GNC-GM [29] with parameters set according

Algorithm 2: IMOT (with noise bound)

Input: measurements $\{\mathbf{m}_i\}_{i=1}^N$, number of layers for Otsu's thresholding d , convergence criterion δ , noise bound (inlier threshold) γ ;

- 1 Run Algorithm 1, and $\mathcal{E} \leftarrow \emptyset$;
- 2 **if** $T^t \geq 5\gamma$ **then**
- 3 Find all measurements whose residual errors are smaller than T^t and gather them into set \mathcal{E} ;
- 4 **for** $p = 1 : 2$ **do**
- 5 Solve the optimal \mathbf{x}^* using the non-minimal solver with the measurements in set \mathcal{E} ;
- 6 Update \mathcal{E} by gathering all the measurements whose residual errors are smaller than $(T^t - \frac{1}{2}p \cdot (T^t - \gamma))$ into set \mathcal{E} ;
- 7 **end**
- 8 **else**
- 9 Find all measurements whose residual errors are smaller than γ and gather them into set \mathcal{E} ;
- 10 Solve the optimal \mathbf{x}^* using the non-minimal solver with the measurements in set \mathcal{E} ;
- 11 **end**
- 12 **return** optimal solution \mathbf{x}^* and inlier set \mathcal{E} ;

to [29], (ii) ADAPT [27] where parameters are set by default as in [1] with 200 maximum iterations, and (iii) RANSAC [12] with 200 maximum iterations and 99% confidence. The experiments are conducted in Matlab on a PC with i7-7700HQ CPU and 16GB RAM using single thread.

A. Single Rotation Averaging

Robust single rotation averaging aims to find the best rotation $\mathbf{R}^* \in SO(3)$ from multiple noise-corrupted estimates w.r.t. a certain rotation which contain potential outliers. Given N rotation matrices $\mathbf{R}_i \in SO(3)$, $i = 1, 2, \dots, N$, the residual error (function) is defined by: $Re_i = dis(\mathbf{R}_i, \mathbf{R}^*)$, where 'dis' is the geodesic distance [13] between rotations.

Experiments. We generate a random ground-truth rotation $\mathbf{R}_{gt} \in SO(3)$ and then generate $N = 100$ noise-corrupted rotations \mathbf{R}_i such that $\mathbf{R}_i = \mathbf{R}_{gt} \text{Exp}(\zeta_i \mathbf{e}_i)$ where ζ_i is a random isotropic Gaussian noise angle with standard deviation $\sigma = 5^\circ$ and \mathbf{e}_i is a random unit-norm 3D vector, as the input measurements in each test. To create outliers, we replace 10%–80% of the rotations in $\{\mathbf{R}_i\}_{i=1}^N$ with random rotations. For the benchmarking, we compare our IMOT and IMOT* with: (i) GNC-TLS and GNC-GM, (ii) ADAPT, and (iii) the recent state-of-the-art Chordal-median and Geodesic-median methods [15]. The noise bound is constantly set as $\gamma = 3\sigma$. In GNC, we use the weighted L1-chordal mean for weighted non-minimal estimation; in ADAPT and IMOT & IMOT*, we use the L1-chordal median [15] as the non-minimal solver. (Here we adopt the open-source experimental setup of [15] for reference).

Results. As illustrated in Fig. 2, we can see that all the tested solvers are robust against up to **70%** of outliers. In terms of time-efficiency, our IMOT & IMOT* are **5–10** times faster than GNC-TLS, **4–8** times faster than GNC-GM and **14–29** times faster than ADAPT (computed with

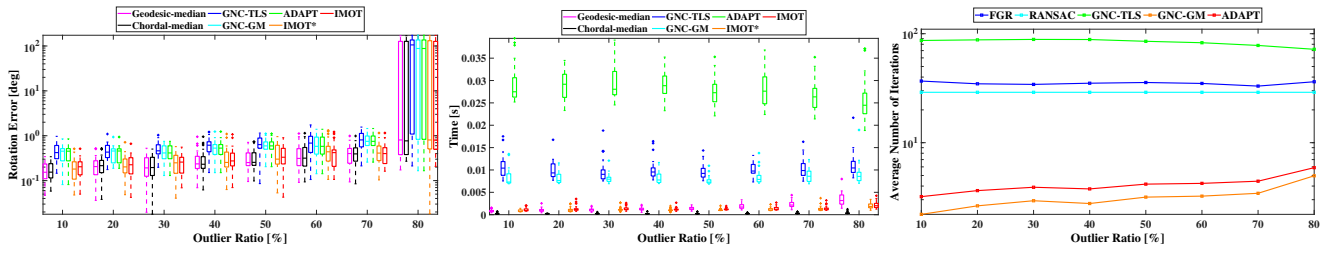
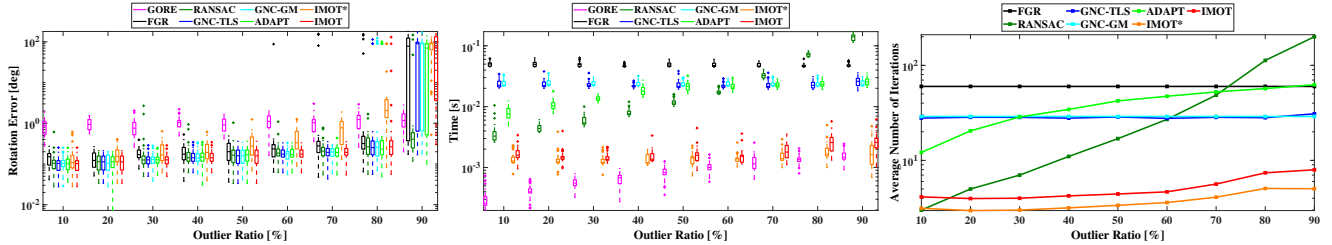


Fig. 2. Benchmarking on Single Rotation Averaging. All data are obtained over 30 Monte Carlo runs.

(a) Limited measurements: $N = 100$



(a) Sufficient measurements: $N = 500$

Fig. 3. Benchmarking on Rotation Search. All data are obtained over 30 Monte Carlo runs.

average runtime), and are also in line with the 2 state-of-the-art specialized methods [15], exhibiting outstanding comprehensive performance.

B. Rotation Search (Wahba’s Problem)

Robust rotation search (also known as the *Wahba’s problem*) is to estimate the best rotation $\mathbf{R}^* \in SO(3)$ that aligns two sets of 3D vectors in the presence of potential outliers. Assume we have N vector correspondences: $\{\mathbf{p}_i \leftrightarrow \mathbf{q}_i\}_{i=1}^N$ ($\mathbf{p}_i, \mathbf{q}_i \in \mathbb{R}^3$, usually normalized to unit length), the residual error can be given by: $Re_i = \|\mathbf{R}^* \mathbf{p}_i - \mathbf{q}_i\|$.

Experiments. In each test, we generate $N = \{100, 500\}$ random unit-norm 3D vectors $\{\mathbf{p}_i\}_{i=1}^N$ to simulate both the measurement-sufficient and measurement-limited situations, rotate $\{\mathbf{p}_i\}_{i=1}^N$ with a random rotation $\mathbf{R}_{gt} \in SO(3)$, and add random isotropic Gaussian noise with $\sigma = 0.01$ to obtain $\{\mathbf{q}_i\}_{i=1}^N$. We corrupt 10%–90% of vectors in $\{\mathbf{q}_i\}_{i=1}^N$ with random 3D vectors as outliers. We benchmark IMOT and IMOT* with: (i) GNC-TLS and GNC-GM, (ii) ADAPT, (iii) RANSAC, (iv) FGR [34] (without translation estimation), and (v) the state-of-the-art GORE [21]. The noise bound is set to $\gamma = 6\sigma$, and we adopt [14] as the minimal solver for RANSAC and use Arun’s SVD method [2] as the standard non-minimal solver.

Results. From Fig. 3, we find that: (i) the robustness of our IMOT & IMOT* is comparable to GNC and ADAPT and superior to FGR, that is, tolerating **70%** outliers with limited measurements and **80%** outliers with sufficient measurements, and (ii) IMOT & IMOT* are more time-efficient than all the other tested solvers except GORE, and specifically

they are **12–18** times faster than GNC, **5–16** times faster than ADAPT and up to over **17–21** times faster than RANSAC in the measurement-limited cases, and are **15–23** times faster than GNC, **13–37** times faster than ADAPT and up to about **50** times faster than RANSAC in the measurement-sufficient cases (all computed with average runtime).

C. Point Cloud Registration

Robust point cloud registration consists in computing the optimal transformation: $\mathbf{R}^* \in SO(3)$ and $\mathbf{t}^* \in \mathbb{R}^3$ aligning two 3D point sets from point correspondences perturbed by outliers. With N correspondences: $\{\mathbf{a}_i \leftrightarrow \mathbf{b}_i\}_{i=1}^N$ ($\mathbf{a}_i, \mathbf{b}_i \in \mathbb{R}^3$ are established by feature matching techniques, e.g. [23]), we can write the residual error as: $Re_i = \|\mathbf{R}^* \mathbf{a}_i + \mathbf{t}^* - \mathbf{b}_i\|$.

Experiments. We use the *bunny* model from Stanford 3D Repository [11] as the point cloud to test on. We downsample the *bunny* to $N = \{100, 1000\}$ points: $\{\mathbf{a}_i\}_{i=1}^N$ (for the measurement-limited and measurement-sufficient cases), and rescale them to fit in a $1^3 m$ cube. In each run, we transform $\{\mathbf{a}_i\}_{i=1}^N$ with a random rigid transformation: $\mathbf{R}_{gt} \in SO(3)$, $\mathbf{t}_{gt} \in \mathbb{R}^3$, and add random zero-mean Gaussian noise with $\sigma = 0.01$ to obtain $\{\mathbf{q}_i\}_{i=1}^N$. Afterwards, 10%–95% of the points in $\{\mathbf{q}_i\}_{i=1}^N$ are replaced by random 3D points to generate outliers. We benchmark IMOT and IMOT* against: (i) GNC-TLS and GNC-GM, (ii) ADAPT, (iii) RANSAC, (iv) FGR, (v) GORE [5], and (vi) the recent state-of-the-art TriVoC [26]. Noise bound is uniformly set to $\gamma = 5\sigma$. We adopt Horn’s triad-based method [14] as RANSAC’s minimal solver and Arun’s SVD [2] as the non-minimal solver.

Results. From Fig. 4, we observe that: (i) IMOT & IMOT*

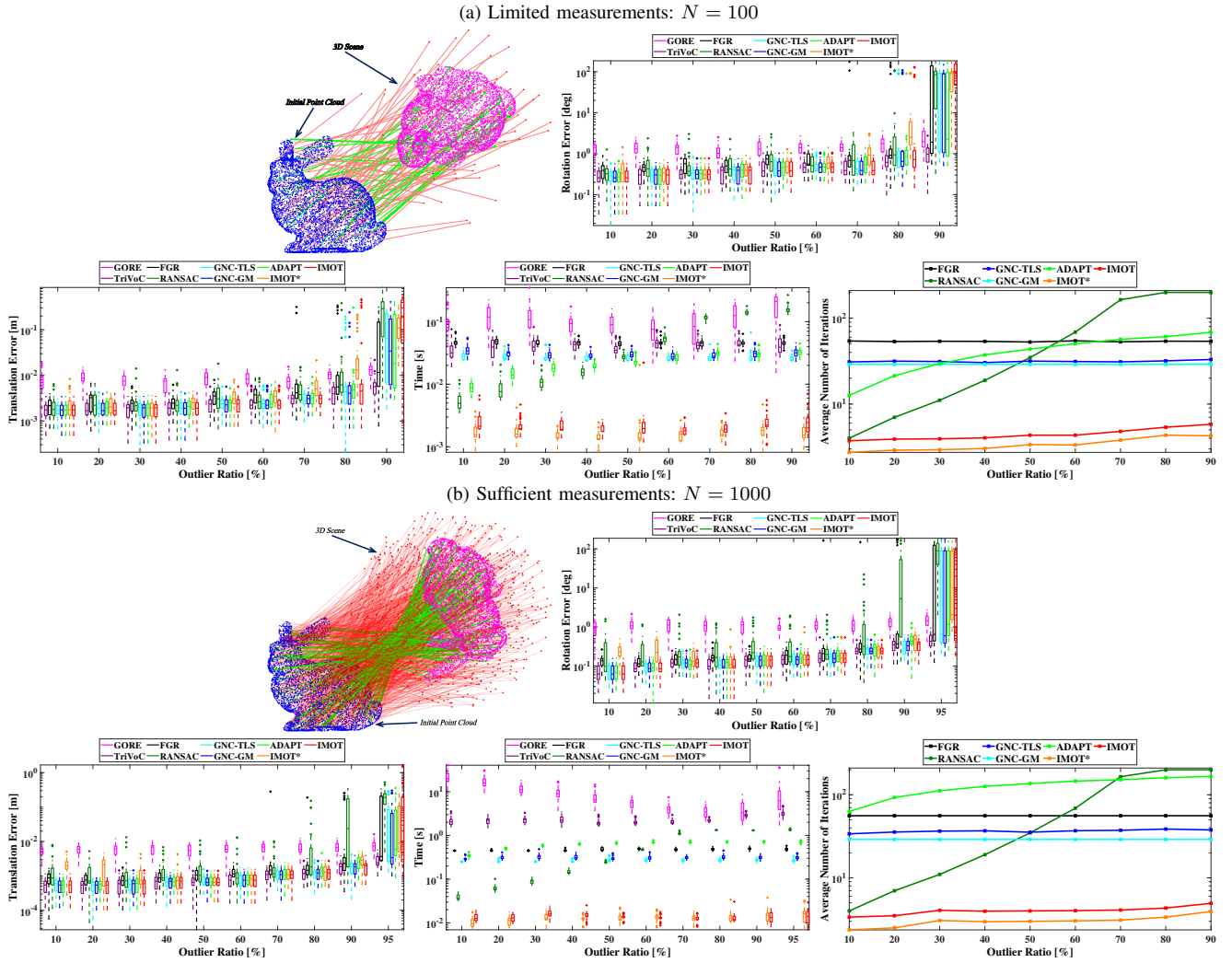


Fig. 4. Benchmarking on Point Cloud Registration. All data are obtained over 30 Monte Carlo runs. The left-top images exemplify the experimental setup in our benchmarking, where green lines denote inlier correspondences and red lines denote outliers.

are robust against **70%** outliers when $N = 100$ and against **90%** outliers when $N = 1000$, comparable to GNC and ADAPT and superior to RANSAC and FGR, yet not as robust as the 2 specialized solvers GORE and TriVoC, and (ii) as for runtime, IMOT & IMOT* are the **fastest** solvers overall, being **9–20** times faster than GNC, **3–19** times faster than ADAPT, and up to **60–70** times faster than RANSAC when $N = 100$, and being **20–27** times faster than GNC, **26–55** times faster than ADAPT, and at most **100** times faster than RANSAC when $N = 1000$ (computed with mean runtime).

D. Category-level Perception

Robust category-level perception seeks to simultaneously estimate the pose: $\mathbf{R}^* \in SO(3)$ and $\mathbf{t}^* \in \mathbb{R}^3$ plus the shape model: $\mathbf{c}^* = [c_1^*, c_2^*, \dots, c_K^*]^T$ of the 3D target object from correspondences established between 3D points $\{\mathbf{y}_i\}_{i=1}^N$ on the object and that on the known CAD models: $\{\mathcal{B}_k\}_{k=1}^K = \{\{\mathbf{b}_k(i)\}_{i=1}^N\}_{k=1}^K$, which are potentially spoiled by outliers. (We borrow the problem definition in [24] where readers can find more details.) The correspondences can be written as: $\{\mathbf{y}_i \leftrightarrow \{\mathbf{b}_k(i)\}_{k=1}^K\}_{i=1}^N$, and the residual error can be given by: $Re_i = \|\mathbf{R}^* \sum_{k=1}^K c_k^* \mathbf{b}_k(i) + \mathbf{t}^* - \mathbf{y}_i\|$.

Experiments. We use the setup in [31] for experimental

benchmarking on category-level perception. Similar to prior tests, we generate 2 classes (measurement limited and sufficient) of the 3D CAD models: $\{\{\mathbf{b}_k(i)\}_{i=1}^N\}_{k=1}^K$ with $N = \{100, 500\}$ and the shape size $K = \{10, 50\}$, respectively. Then, in each test, we create random points as the CAD models and a random pose to transform these models and then add zero-mean Gaussian noise with $\sigma = 0.01$ on them to create the object points: $\{\mathbf{y}_i\}_{i=1}^N$. We apply the certifiably optimal solution in [24] to be the non-minimal solver, and compare our IMOT & IMOT* with GNC-TLS, GNC-GM and ADAPT.

Results. According to Fig. 5, GNC, ADAPT and our IMOT & IMOT* all display **70%-80%** of outlier-robustness, whereas IMOT & IMOT* apparently exceeds the other estimators in terms of the solution speed, that is, **4–9** times faster than GNC and **4–15** times faster than ADAPT when $N = 100$ and $K = 10$, and **6–11** times faster than GNC and **14–45** times faster than ADAPT when $N = 500$ and $K = 50$ (computed with average runtime). Despite the superiority of our proposed solvers, IMOT* generates relatively high estimation error (sometimes exceeding 1° in rotation error) when $N = 100$ and $K = 10$.

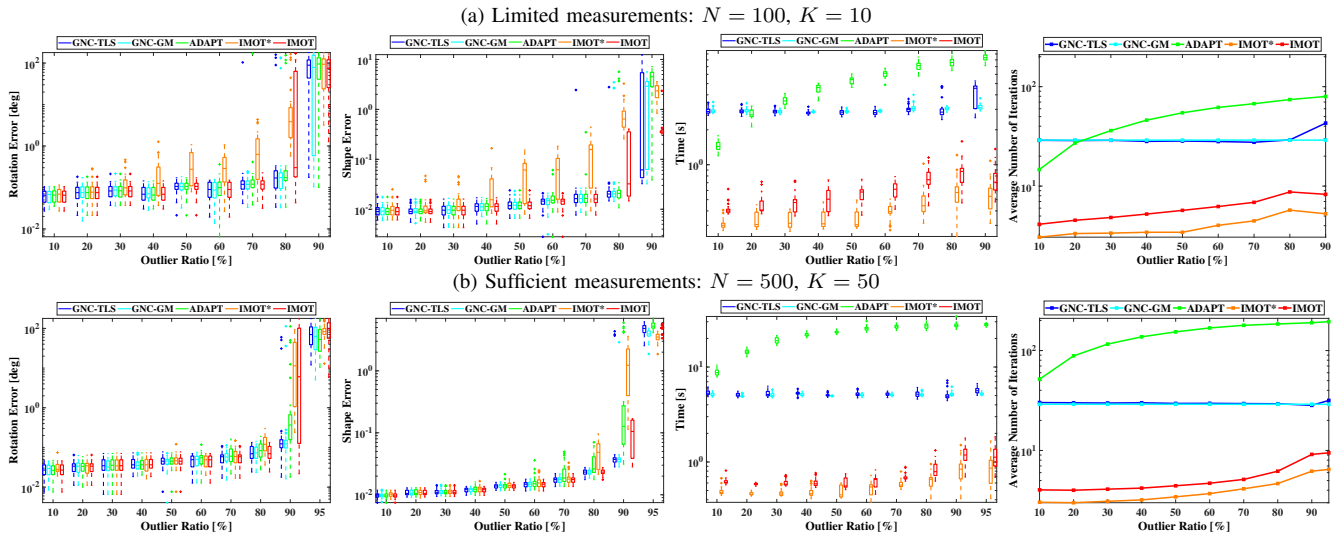


Fig. 5. Benchmarking on Category-level Perception. All data are obtained over 30 Monte Carlo runs. Translation errors are omitted here they are rather similar to the rotation and shape errors.

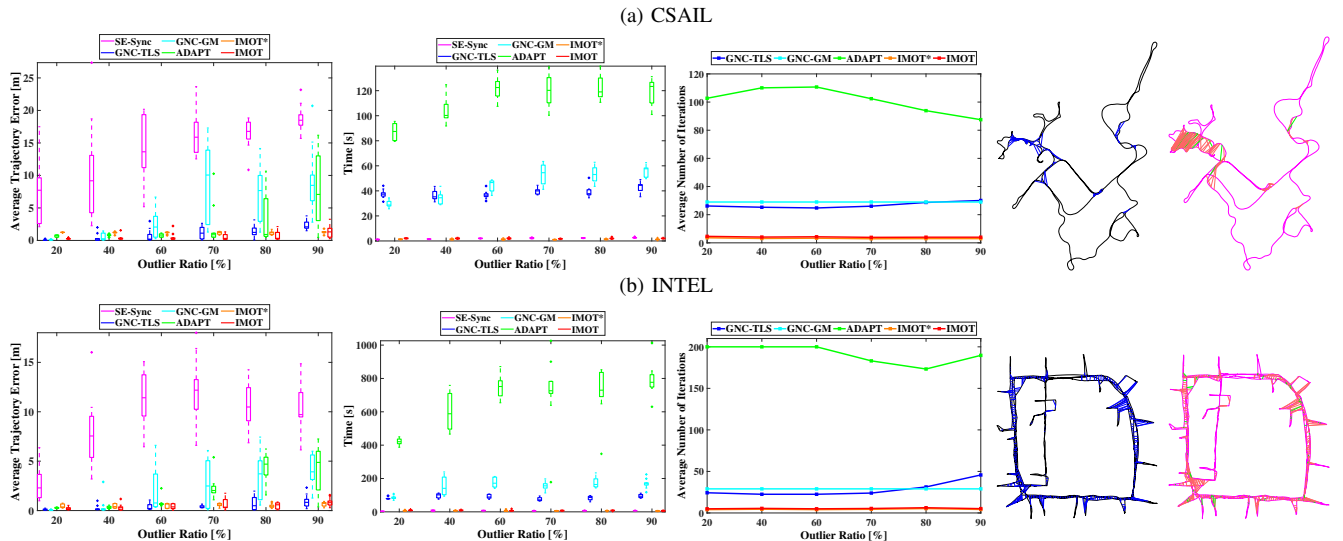


Fig. 6. Benchmarking on SLAM. All data are obtained over 10 Monte Carlo runs. Images in the right most column exemplify the quantitative results on SLAM problems with 90% outliers, where the left images show the ground-truth trajectories in black (with blue lines denoting loop-closures) and the right images show the trajectories estimated by IMOT in magenta (with green lines denoting inlier loop-closures and red ones denoting outliers).

E. SLAM (Pose Graph Optimization)

Robust SLAM (pose graph optimization) needs to optimize a sequence of robot or camera poses $\{(\mathbf{R}_j^*, \mathbf{t}_j^*)\}_{j=1}^M$ on a trajectory using the known relative pose relations: $(\mathbf{R}_{jk}^o, \mathbf{t}_{jk}^o)$ (where $j, k \in \{1, 2, \dots, M\}$) between the consecutive poses (odometry measurements) or non-consecutive poses (loop-closure measurements), where the latter could be contaminated by outliers. And the residual error w.r.t. a certain pair of poses can be formulated as: $Re_{jk} = \sqrt{\frac{\omega_{jk}^R}{2} \|\mathbf{R}_j - \mathbf{R}_k \mathbf{R}_{jk}^o\|_F^2 + \omega_{jk}^t \|\mathbf{t}_j - \mathbf{t}_k - \mathbf{R}_k \mathbf{t}_{jk}^o\|_2^2}$, where ω_{jk}^R and ω_{jk}^t are noise-distribution parameters [7] and ‘ $\|\cdot\|_F$ ’ indicates the Frobenius norm.

Experiments. We conduct the benchmarking tests on the CSAIL and INTEL datasets from the open-source package of [22]. To simulate outliers, we keep the odometry measurements (that are generally considered as the correct measurements) and corrupt a portion of the loop-closures (randomly chosen) with random poses, similar to the setup

in [29]. We use SE-Sync [22] as the non-minimal solver, and compare IMOT & IMOT* with GNC and ADAPT.

Since we find IMOT & IMOT* cannot work well if using all the measurements (odometry and loop-closures) directly as the input, we only take the odometry measurements for non-minimal estimation in the first iteration of IMOT & IMOT*. (In fact, IMOT&IMOT* are applicable on the condition that odometry measurements are generally reliable).

Results. As shown in Fig. 6, for CSAIL, GNC-TLS and our IMOT & IMOT* can tolerate up to **90%** outliers (with acceptable trajectory error), while GNC-GM and ADAPT breaks at 70%, and more importantly, IMOT & IMOT* are **14–39** times faster than GNC and **41–119** times faster than ADAPT. In terms of INTEL, GNC-TLS and our IMOT & IMOT* remain robust against up to **90%** outliers, whereas GNC-GM and ADAPT cannot make promising estimates when the outlier ratio grows over 60%–70%. Furthermore, IMOT & IMOT* are **9–36** times faster than GNC and **45–125** times faster than ADAPT.

V. CONCLUSION

A general-purpose, fast, deterministic and outlier-robust estimator is rendered in this paper. By embedding a multi-layered thresholding technique based on Otsu's method into an iterative measurement-grouping framework, we propose our estimator IMOT to effectively robustify standard non-minimal solvers for a variety of spatial perception problems. Through experiments on diverse applications, we show that our estimator can converge mostly in fewer than 10 iterations, which is several to dozens of (even more than a hundred) times faster than GNC and/or ADAPT, while showing similarly state-of-the-art (70%–90%) robustness. Considering the probably slow runtime of non-minimal solvers, our estimator can be a promising alternate method for GNC and ADAPT in some cases. Also, it does not necessarily rely on the noise bound as input, making its application flexible.

The main drawback of our estimator is: it may not be applicable when the input measurement number is too small (e.g. < 20) since the multi-layered thresholding strategy achieves fast convergence at the cost of keeping only a small portion of measurements in each iteration. Once the measurement number in one lower-residual group is lower than the smallest number required by the non-minimal solver, robust estimation could fail. Thus, IMOT is suggested to be used in situations with not-too-sparse measurements. Besides, IMOT cannot deal with SLAM problems where odometry measurements are very unreliable.

REFERENCES

- [1] Pasquale Antonante, Vasileios Tzoumas, Heng Yang, and Luca Carlone. Outlier-robust estimation: Hardness, minimally tuned algorithms, and applications. *IEEE Transactions on Robotics*, 2021.
- [2] K Somani Arun, Thomas S Huang, and Steven D Blostein. Least-squares fitting of two 3-d point sets. *IEEE Transactions on pattern analysis and machine intelligence*, (5):698–700, 1987.
- [3] Gérard Blais and Martin D. Levine. Registering multiview range data to create 3d computer objects. *IEEE Transactions on Pattern Analysis and Machine Intelligence*, 17(8):820–824, 1995.
- [4] Jesus Briales and Javier Gonzalez-Jimenez. Convex global 3d registration with lagrangian duality. In *Proceedings of the IEEE Conference on Computer Vision and Pattern Recognition*, pages 4960–4969, 2017.
- [5] Alvaro Parra Bustos and Tat-Jun Chin. Guaranteed outlier removal for point cloud registration with correspondences. *IEEE transactions on pattern analysis and machine intelligence*, 40(12):2868–2882, 2017.
- [6] Cesar Cadena, Luca Carlone, Henry Carrillo, Yasir Latif, Davide Scaramuzza, José Neira, Ian Reid, and John J Leonard. Past, present, and future of simultaneous localization and mapping: Toward the robust-perception age. *IEEE Transactions on robotics*, 32(6):1309–1332, 2016.
- [7] Luca Carlone and Giuseppe C Calafiore. Convex relaxations for pose graph optimization with outliers. *IEEE Robotics and Automation Letters*, 3(2):1160–1167, 2018.
- [8] Sungjoon Choi, Qian-Yi Zhou, and Vladlen Koltun. Robust reconstruction of indoor scenes. In *Proceedings of the IEEE Conference on Computer Vision and Pattern Recognition*, pages 5556–5565, 2015.
- [9] Ondrej Chum and Jiri Matas. Matching with prosac-progressive sample consensus. In *2005 IEEE computer society conference on computer vision and pattern recognition (CVPR'05)*, volume 1, pages 220–226. IEEE, 2005.
- [10] Ondřej Chum, Jiří Matas, and Josef Kittler. Locally optimized ransac. In *Joint Pattern Recognition Symposium*, pages 236–243. Springer, 2003.
- [11] Brian Curless and Marc Levoy. A volumetric method for building complex models from range images. In *Proceedings of the 23rd annual conference on Computer graphics and interactive techniques*, pages 303–312, 1996.
- [12] Martin A Fischler and Robert C Bolles. Random sample consensus: a paradigm for model fitting with applications to image analysis and automated cartography. *Communications of the ACM*, 24(6):381–395, 1981.
- [13] Richard Hartley, Jochen Trunpf, Yuchao Dai, and Hongdong Li. Rotation averaging. *International journal of computer vision*, 103(3):267–305, 2013.
- [14] Berthold KP Horn. Closed-form solution of absolute orientation using unit quaternions. *Josa a*, 4(4):629–642, 1987.
- [15] Seong Hun Lee and Javier Civera. Robust single rotation averaging. *arXiv preprint arXiv:2004.00732*, 2020.
- [16] Hongdong Li. Consensus set maximization with guaranteed global optimality for robust geometry estimation. In *2009 IEEE 12th International Conference on Computer Vision*, pages 1074–1080. IEEE, 2009.
- [17] Kirk MacTavish and Timothy D Barfoot. At all costs: A comparison of robust cost functions for camera correspondence outliers. In *2015 12th conference on computer and robot vision*, pages 62–69. IEEE, 2015.
- [18] F Landis Markley and John L Crassidis. Fundamentals of spacecraft attitude determination and control. 2014.
- [19] David Nistér. An efficient solution to the five-point relative pose problem. *IEEE transactions on pattern analysis and machine intelligence*, 26(6):756–770, 2004.
- [20] Nobuyuki Otsu. A threshold selection method from gray-level histograms. *IEEE transactions on systems, man, and cybernetics*, 9(1):62–66, 1979.
- [21] Alvaro Parra Bustos and Tat-Jun Chin. Guaranteed outlier removal for rotation search. In *Proceedings of the IEEE International Conference on Computer Vision*, pages 2165–2173, 2015.
- [22] David M Rosen, Luca Carlone, Afonso S Bandeira, and John J Leonard. Se-sync: A certifiably correct algorithm for synchronization over the special euclidean group. *The International Journal of Robotics Research*, 38(2-3):95–125, 2019.
- [23] Radu Bogdan Rusu, Nico Blodow, and Michael Beetz. Fast point feature histograms (fpfh) for 3d registration. In *2009 IEEE international conference on robotics and automation*, pages 3212–3217. IEEE, 2009.
- [24] Jingnan Shi, Heng Yang, and Luca Carlone. Optimal pose and shape estimation for category-level 3d object perception. *Robotics: Science and Systems (RSS)*, 2021.
- [25] Lei Sun. Ransic: Fast and highly robust estimation for rotation search and point cloud registration using invariant compatibility. *IEEE Robotics and Automation Letters*, 7(1):143–150, 2022.
- [26] Lei Sun and Lu Deng. Trivoc: Efficient voting-based consensus maximization for robust point cloud registration with extreme outlier ratios. *IEEE Robotics and Automation Letters*, 2022.
- [27] Vasileios Tzoumas, Pasquale Antonante, and Luca Carlone. Outlier-robust spatial perception: Hardness, general-purpose algorithms, and guarantees. In *2019 IEEE/RSJ International Conference on Intelligent Robots and Systems (IROS)*, pages 5383–5390. IEEE, 2019.
- [28] Jay M Wong, Vincent Kee, Tiffany Le, Syler Wagner, Gian-Luca Mariottini, Abraham Schneider, Lei Hamilton, Rahul Chipalkatty, Mitchell Hebert, David MS Johnson, et al. Segicp: Integrated deep semantic segmentation and pose estimation. In *2017 IEEE/RSJ International Conference on Intelligent Robots and Systems (IROS)*, pages 5784–5789. IEEE, 2017.
- [29] Heng Yang, Pasquale Antonante, Vasileios Tzoumas, and Luca Carlone. Graduated non-convexity for robust spatial perception: From non-minimal solvers to global outlier rejection. *IEEE Robotics and Automation Letters*, 5(2):1127–1134, 2020.
- [30] Heng Yang and Luca Carlone. In perfect shape: Certifiably optimal 3d shape reconstruction from 2d landmarks. In *Proceedings of the IEEE/CVF Conference on Computer Vision and Pattern Recognition*, pages 621–630, 2020.
- [31] Heng Yang and Luca Carlone. Certifiably outlier-robust geometric perception: Exact semidefinite relaxations and scalable global optimization. *arXiv preprint arXiv:2109.03349*, 2021.
- [32] Andy Zeng, Kuan-Ting Yu, Shuran Song, Daniel Suo, Ed Walker, Alberto Rodriguez, and Jianxiong Xiao. Multi-view self-supervised deep learning for 6d pose estimation in the amazon picking challenge. In *2017 IEEE international conference on robotics and automation (ICRA)*, pages 1386–1383. IEEE, 2017.
- [33] Ji Zhang and Sanjiv Singh. Visual-lidar odometry and mapping: Low-drift, robust, and fast. In *2015 IEEE International Conference on Robotics and Automation (ICRA)*, pages 2174–2181. IEEE, 2015.
- [34] Qian-Yi Zhou, Jaesik Park, and Vladlen Koltun. Fast global registration. In *European Conference on Computer Vision*, pages 766–782. Springer, 2016.